

Hydrodynamics for heavy-ion collisions – status and recent developments –

Ulrich Heinz



THE OHIO STATE UNIVERSITY

Theoretical Physics Colloquium, 26 May 2021

Largely based on work done by my students and postdocs:

**Dennis Bazow, Chandroday Chattopadhyay, Lipei Du, Derek Everett,
Kevin Ingles, Dan Liyanage, Mauricio Martinez, Mike McNelis**

Many Thanks!

1 Overview

2 Dynamical initialization

3 Violation of boost-invariance

4 Baryon flow and baryon diffusion

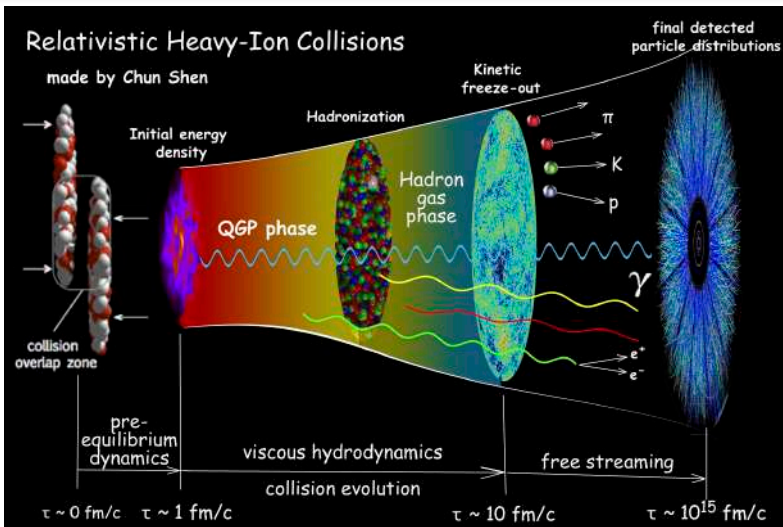
5 Comparison with SPS and RHIC BES data

6 Hydro with critical fluctuations

7 Conclusions

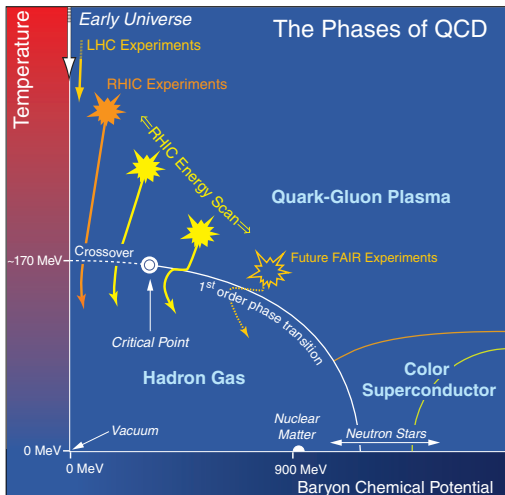
Overview

The Little Bang



credit: Chun Shen

Exploring the QCD phase diagram with heavy-ion collisions



Focus on:

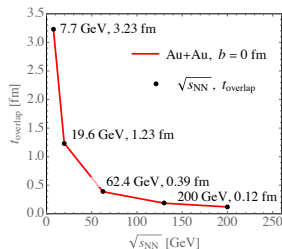
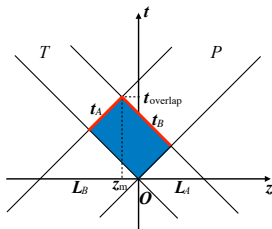
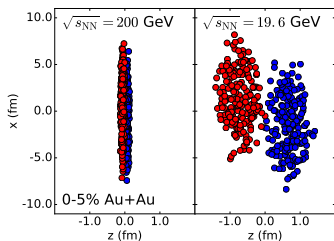
Additional complexities when modeling heavy-ion collisions at lower energies:

- nontrivial interpenetration and energy deposition dynamics;
- (3+1)-d, broken boost-invariance;
- equation of state (EoS) at zero strangeness but nonzero electric and baryon charges;
- (non-equilibrium) dynamics of conserved charges: B, Q, S;
- QCD critical point: dynamics of critical fluctuations and correlations (“critical slow modes”);
- hydrodynamization of fluctuations;
- back-reaction of non-equilibrium fluctuations on bulk dynamics
- ...

Dynamical initialization

Initial conditions: (3+1)-d dynamical initialization

Collision geometry and maximum overlap time in Au-Au collisions [Shen & Schenke 1710.00881, Du et al. 1807.04721]



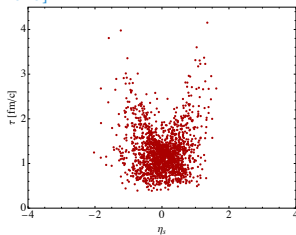
- At RHIC BES energies, the space-time history of nuclear interpenetration and energy deposition is complicated and depends on transverse position;
- Hydrodynamic initial conditions have a complex (3+1)-d structure;
- **Challenges:**
 - large model uncertainties, especially for baryon stopping [Denicol et al. 1804.10557; Bialas et al. 1608.07041; Du et al. 1807.04721; Shen & Schenke 1710.00881];
 - dynamical interface between (3+1)-d pre-hydrodynamics and hydrodynamics [Shen & Schenke 1710.00881; Akamatsu et al. 1805.09024; Kanakubo et al. 1806.10329].

Initial conditions: (3+1)-d dynamical initialization

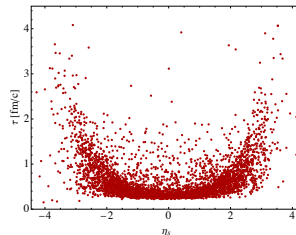
Energy deposition in central Au-Au collisions

UrQMD [Du QM2018]

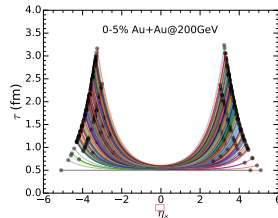
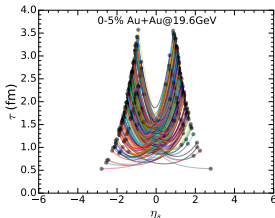
AuAu @ 19.6 GeV b=0 fm



AuAu @ 200 GeV b=0 fm



String model [Shen & Schenke 1710.00881]



Conservation laws and source terms

The conservation laws are

$$d_\mu T^{\mu\nu} = d_\mu \left[T_{\text{fluid}}^{\mu\nu} + T_{\text{particle}}^{\mu\nu} \right] = 0 ,$$

$$d_\mu N^\mu = d_\mu \left[N_{\text{fluid}}^\mu + N_{\text{particle}}^\mu \right] = 0 ,$$

from which we can get the **source terms** for the fluid as

$$d_\mu T_{\text{fluid}}^{\mu\nu} = J_{\text{source}}^\nu(x) \equiv -d_\mu T_{\text{particle}}^{\mu\nu}(x) ,$$

$$d_\mu N_{\text{fluid}}^\mu = \rho_{\text{Bsource}}(x) \equiv -d_\mu N_{\text{particle}}^\mu(x) .$$

Source terms and thermalization

Baryon current and energy-momentum tensor of the particles are given by [D. Oliinychenko and H. Petersen, [Phys.Rev. C93 \(2016\) 034905](#)]

$$T_{\text{particle}}^{\mu\nu}(t, \mathbf{r}) = \sum_i \frac{p_i^\mu p_i^\nu}{p_i^0} K(\mathbf{r} - \mathbf{r}_i(t), p_i) ,$$

$$N_{\text{particle}}^\mu(t, \mathbf{r}) = \sum_i b_i \frac{p_i^\mu}{p_i^0} K(\mathbf{r} - \mathbf{r}_i(t), p_i) .$$

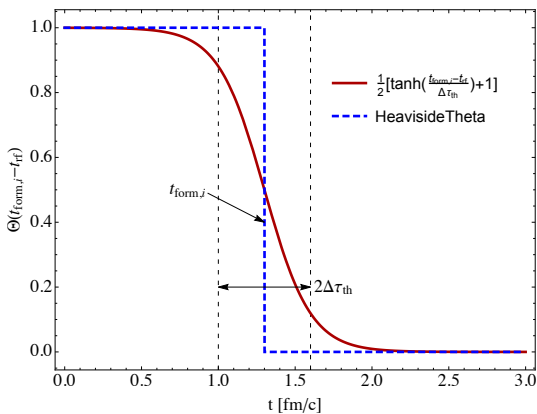
The [smearing kernel](#) in the rest frame is given by

$$K_i(t_{\text{rf}}, \mathbf{x}_{\text{rf}}, p_i) = \gamma_i \frac{1}{(2\pi\sigma^2)^{3/2}} \exp \left[\frac{-(\mathbf{x}_{\text{rf}} - \mathbf{r}_{\text{rf},i})^2}{2\sigma^2} \right] \Theta(t_{\text{form},i} - t_{\text{rf}}),$$

$$\equiv \gamma_i \frac{1}{(2\pi\sigma^2)^{3/2}} \exp \left[\frac{(x - x_i(t))^2 - (u_i \cdot (x - x_i(t)))^2}{2\sigma^2} \right] \Theta(t_{\text{form},i} - t_{\text{rf}}).$$

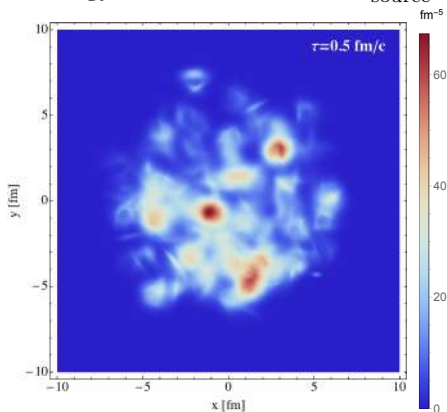
Source terms and thermalization

$$\Theta(t_{\text{form}} - t) = \frac{1}{2} \left[\tanh \left(\frac{t_{\text{form}} - t}{\Delta\tau_{\text{th}}} \right) + 1 \right] \xrightarrow{\Delta\tau_{\text{th}} \rightarrow 0} \theta(t_{\text{form}} - t).$$

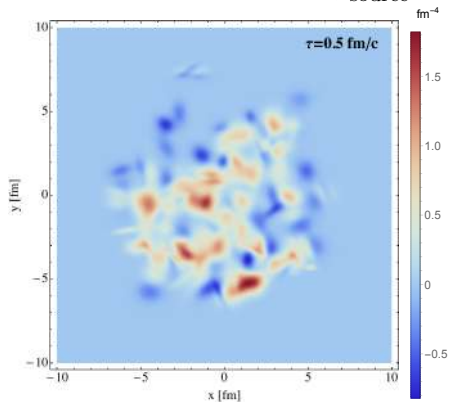


Dynamical sources (illustration for central Au+Au @ 200 A GeV)

Energy-momentum source J_{source}^T



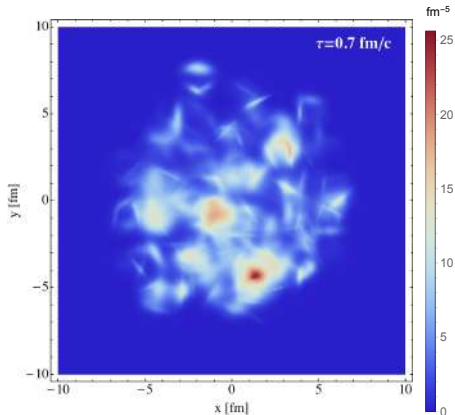
Baryon number source ρ_{source}^B



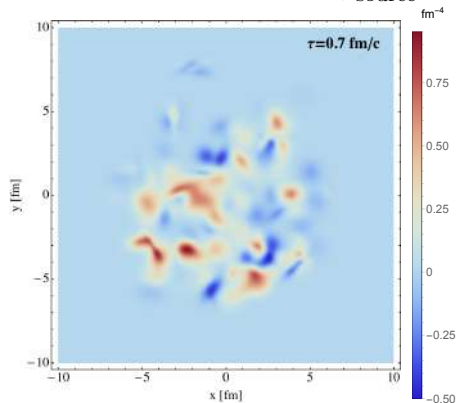
$$\tau = 0.5 \text{ fm}/c$$

Dynamical sources (illustration for central Au+Au @ 200 A GeV)

Energy-momentum source J_{source}^T



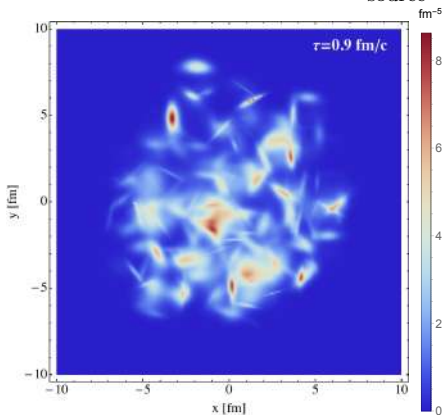
Baryon number source ρ_{source}^B



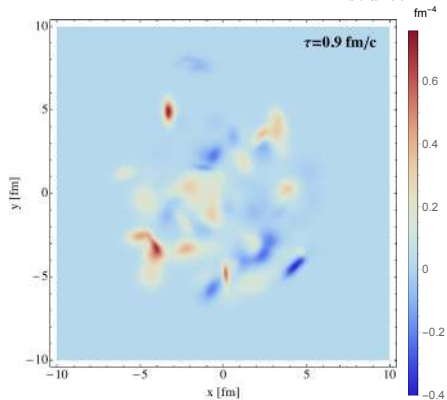
$\tau = 0.7 \text{ fm}/c$

Dynamical sources (illustration for central Au+Au @ 200 A GeV)

Energy-momentum source J_{source}^τ



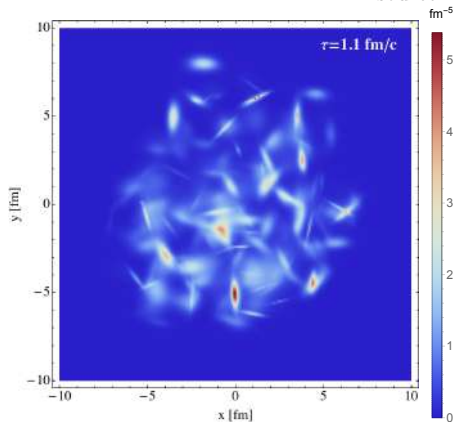
Baryon number source ρ_{source}^B



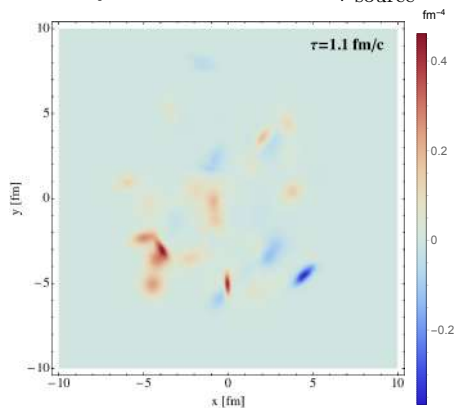
$\tau = 0.9 \text{ fm/c}$

Dynamical sources (illustration for central Au+Au @ 200 A GeV)

Energy-momentum source J_{source}^{τ}



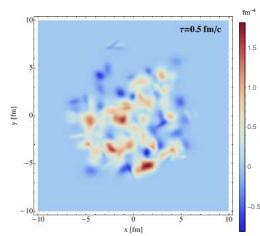
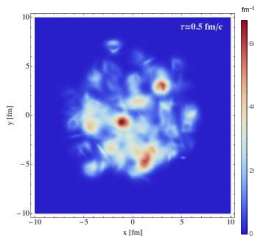
Baryon number source ρ_{source}^B



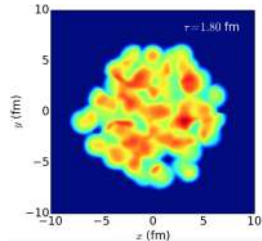
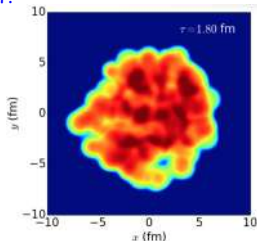
$\tau = 1.1 \text{ fm/c}$

Evolution in the transverse plane (snapshots, central Au+Au @ 200 A GeV)

L. Du, QM2018:



C. Shen, QM2017:

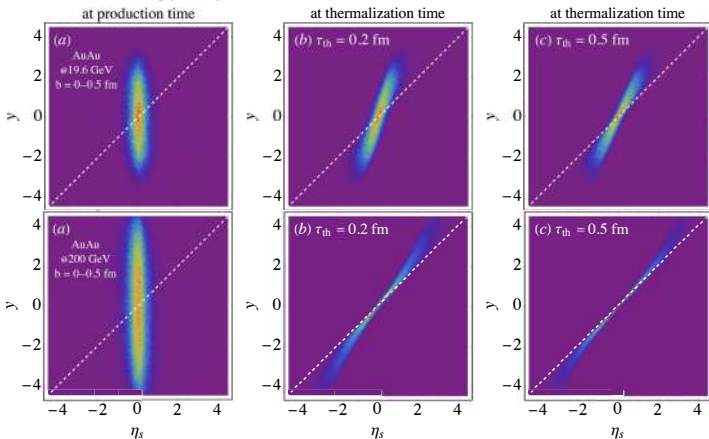


- In our model [Du QM2018], bumpiness of ρ_B is not correlated with that of e

Violation of boost-invariance

Initial longitudinal profiles for energy density

At BES energies, initial energy deposition in UrQMD is not boost-invariant: [Du & UH in preparation]

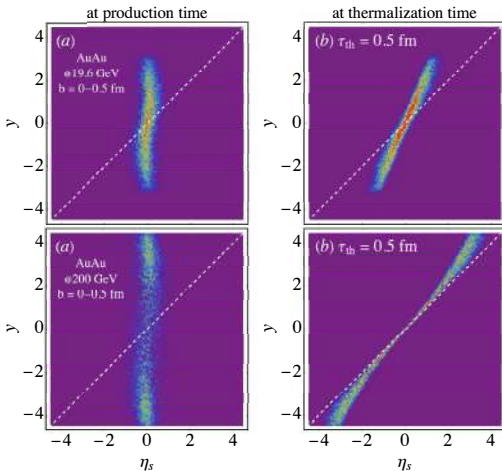


- Initial distribution evolves towards boost-invariance by longitudinal free-streaming
- This evolution is faster at higher collision energies
- Large uncertainty in hydrodynamic initial conditions related to thermalization (formation) time

Initial longitudinal profiles for net baryon number density

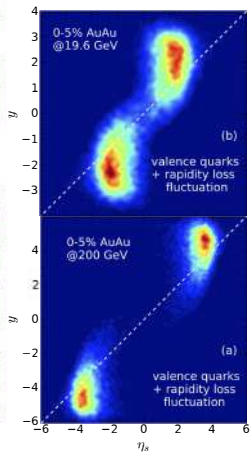
UrQMD initial conditions

[Du & UH in preparation]



String model initial conditions

[Shen & Schenke 1710.00881]



- Large model uncertainties in hydrodynamic initial conditions, especially for the net baryon density distribution!

Baryon flow and diffusion

Baryon flow and baryon diffusion

Conservation laws for energy, momentum and the conserved charges (w/o dynamical initialization):

$$\begin{aligned}d_{\mu} T^{\mu\nu} &= 0, & \text{with } T^{\mu\nu} &= \mathcal{E} u^{\mu} u^{\nu} - (\mathcal{P}_{\text{eq}} + \Pi) \Delta^{\mu\nu} + \pi^{\mu\nu}, \\d_{\mu} N_i^{\mu} &= 0, & \text{with } N_i^{\mu} &= \mathcal{N}_i u^{\mu} + n_i^{\mu} \quad (i = B, Q, S).\end{aligned}$$

Baryon flow and baryon diffusion

Conservation laws for energy, momentum and the conserved charges (w/o dynamical initialization):

$$d_\mu T^{\mu\nu} = 0, \quad \text{with } T^{\mu\nu} = \mathcal{E} u^\mu u^\nu - (\mathcal{P}_{\text{eq}} + \Pi) \Delta^{\mu\nu} + \pi^{\mu\nu},$$

$$d_\mu N_i^\mu = 0, \quad \text{with } N_i^\mu = \mathcal{N}_i u^\mu + n_i^\mu \quad (i = B, Q, S).$$

Required ingredients:

- Equation of State (EoS) $\mathcal{P}_{\text{eq}}(\mathcal{E}, \mathcal{N})$

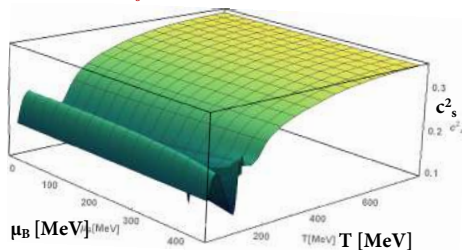
- At non-zero densities for (multiple) conserved charges:

[Monnai et al. 1902.05095; Noronha-Hostler et al. 1902.06723]

- With a critical point:

[P. Parotto et al. 1805.05249]

c_s^2 from an LQCD-based EoS with a CP



[P. Parotto et al., 1805.05249]

Baryon flow and baryon diffusion

Conservation laws for energy, momentum and the conserved charges (w/o dynamical initialization):

$$d_\mu T^{\mu\nu} = 0, \quad \text{with } T^{\mu\nu} = \mathcal{E} u^\mu u^\nu - (\mathcal{P}_{\text{eq}} + \Pi)\Delta^{\mu\nu} + \pi^{\mu\nu},$$

$$d_\mu N_i^\mu = 0, \quad \text{with } N_i^\mu = \mathcal{N}_i u^\mu + n_i^\mu \quad (i = B, Q, S).$$

Required ingredients:

- Equation of State (EoS) $\mathcal{P}_{\text{eq}}(\mathcal{E}, \mathcal{N})$

- At non-zero densities for (multiple) conserved charges:

[Monnai et al. 1902.05095; Noronha-Hostler et al. 1902.06723]

- With a critical point:

[P. Parotto et al. 1805.05249]

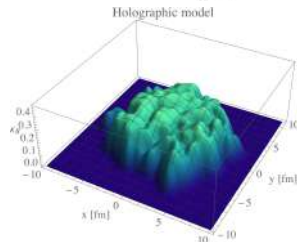
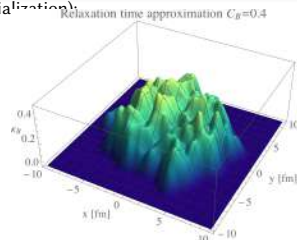
- Transport coefficients

- Shear and bulk viscosity $(\eta/s)(\mu, T), (\zeta/s)(\mu, T)$:

e.g. [Noronha-Hostler et al. 0811.1571; Denicol et al. 1512.01538; Soloveva et al. 1911.08547]

- Diffusion coefficient matrix $\kappa_{ij}(\mu, T)$:

e.g. [Denicol et al. 1804.10557; Rougemont et al. 1507.06972; Fotakis et al. 1912.09103, 2102.08140]



Baryon diffusion coefficients κ_B
from kinetic theory and holography

Baryon flow and baryon diffusion

Conservation laws for energy, momentum and the conserved charges (w/o dynamical initialization):

$$d_\mu T^{\mu\nu} = 0, \quad \text{with } T^{\mu\nu} = \mathcal{E} u^\mu u^\nu - (\mathcal{P}_{\text{eq}} + \Pi)\Delta^{\mu\nu} + \pi^{\mu\nu},$$

$$d_\mu N_i^\mu = 0, \quad \text{with } N_i^\mu = \mathcal{N}_i u^\mu + n_i^\mu \quad (i = B, Q, S).$$

Required ingredients:

Equation of State (EoS) $\mathcal{P}_{\text{eq}}(\mathcal{E}, \mathcal{N})$

- At non-zero densities for (multiple) conserved charges:

[Monnai et al. 1902.05095; Noronha-Hostler et al. 1902.06723]

- With a critical point:

[P. Parotto et al. 1805.05249]

Transport coefficients

- Shear and bulk viscosity $(\eta/s)(\mu, T)$, $(\zeta/s)(\mu, T)$:

e.g. [Noronha-Hostler et al. 0811.1571; Denicol et al. 1512.01538; Soloveva et al. 1911.08547]

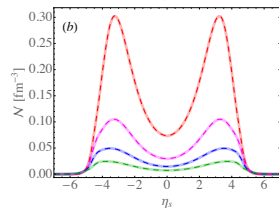
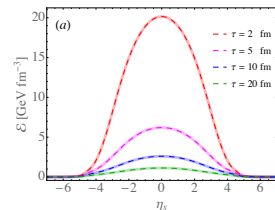
- Diffusion coefficient matrix $\kappa_{ij}(\mu, T)$:

e.g. [Denicol et al. 1804.10557; Rougemont et al. 1507.06972; Fotakis et al. 1912.09103, 2102.08140]

(3+1)-d hydrodynamic simulation with (multiple) conserved currents:

- MUSIC [Denicol et al. 1804.10557]

- BESHYDRO [Du & UH 1906.11181]



(1+1)D comparison between MUSIC and BESHYDRO [Du & UH 1906.11181], both using DNMR theory

[Denicol et al. 1004.5013, 1202.4551]

Hydrodynamic code validation

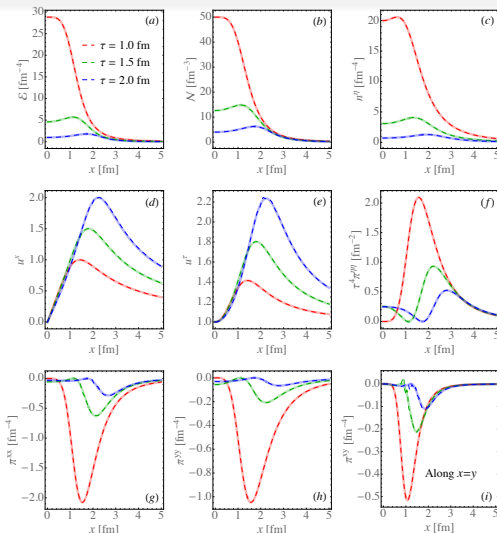
Code validation is essential:

- for quantitative work need to monitor where the code reaches its limits
- numerical precision must not be limiting factor in model-data comparison

Hydrodynamic code validation

Code validation is essential:

- for quantitative work need to monitor where the code reaches its limits
- numerical precision must not be limiting factor in model-data comparison
- example: Gubser flow for testing transverse evolution

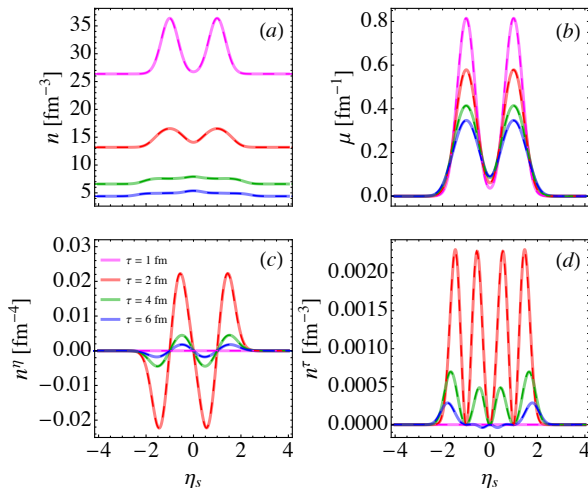


Test of transverse evolution with Gubser flow [Du & UH 1906.11181]

Hydrodynamic code validation

Code validation is essential:

- for quantitative work need to monitor where the code reaches its limits
- numerical precision must not be limiting factor in model-data comparison
- example: Gubser flow for testing transverse evolution
- example: (1+1)-d test for longitudinal evolution of baryon flow and diffusion dynamics w/o transverse gradients

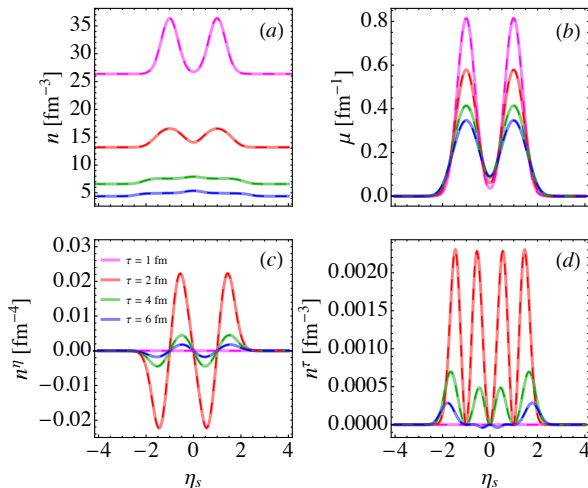


Test of longitudinal evolution [Du, et al. in preparation]

Hydrodynamic code validation

Code validation is essential:

- for quantitative work need to monitor where the code reaches its limits
- numerical precision must not be limiting factor in model-data comparison
- example: Gubser flow for testing **transverse evolution**
- example: (1+1)-d test for **longitudinal evolution of baryon flow and diffusion dynamics** w/o transverse gradients
- for **additional validation protocols** (which can also be used for other codes) see [▶ on GitHub](#)



Test of longitudinal evolution [Du, et al. in preparation]

BESHYDRO documentation



Physics, internal workings and validation schemes are well documented:

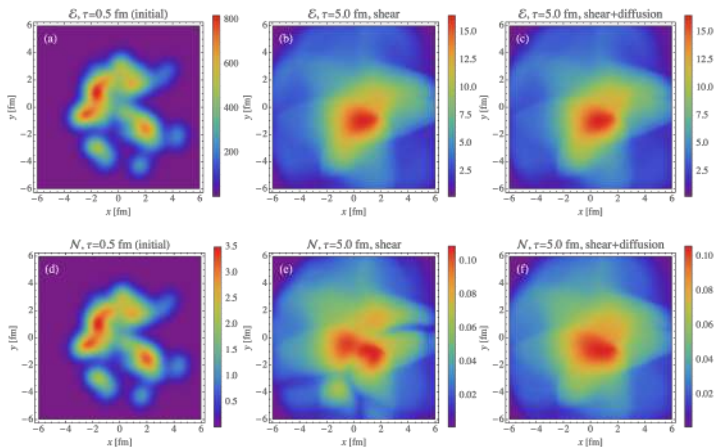
- BESHYDRO paper [Du & UH 1906.11181]
- User manual [▶ on GitHub](#)

Detailed documentation and validation protocols for BESHYDRO allow to explore the inner workings of the hydrodynamic code, by selectively turning on and off (or adding additional) terms describing specific physics mechanisms.

Baryon diffusion smoothes baryon density gradients

- Relaxation equation for baryon diffusion current: $u^\nu \partial_\nu n^\mu = -\frac{1}{\tau_n} \left[n^\mu - \kappa_B \nabla^\mu \left(\frac{\mu}{T} \right) \right] + \dots$

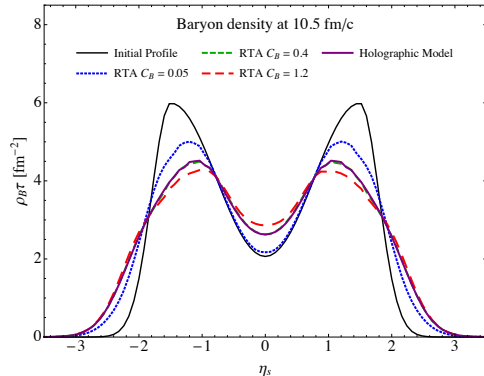
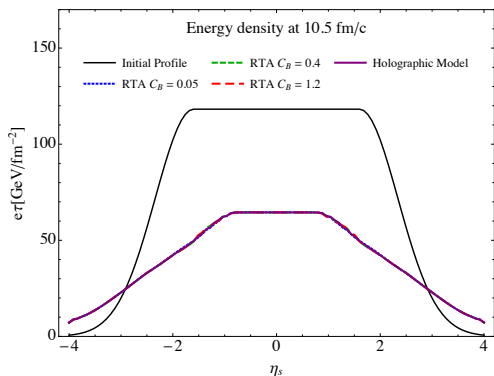
Baryon diffusion coefficient $\kappa_B \propto C_B$ controls response of the diffusion current to the driving force.



Baryon diffusion smoothes baryon density gradients

- Relaxation equation for baryon diffusion current: $u^\nu \partial_\nu n^\mu = -\frac{1}{\tau_n} \left[n^\mu - \kappa_B \nabla^\mu \left(\frac{\mu}{T} \right) \right] + \dots$

Baryon diffusion coefficient $\kappa_B \propto C_B$ controls response of the diffusion current to the driving force.



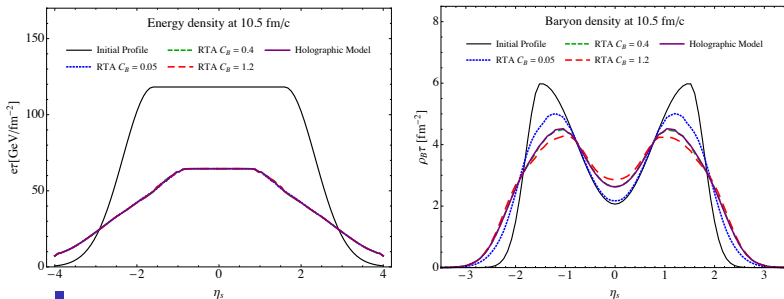
Energy and baryon evolution in longitudinal direction [Du et al. 1807.04721]

Toy model initial state profile from [Denicol et al. 1804.10557]

Baryon diffusion smoothes baryon density gradients

- Relaxation equation for baryon diffusion current: $u^\nu \partial_\nu n^\mu = -\frac{1}{\tau_n} \left[n^\mu - \kappa_B \nabla^\mu \left(\frac{\mu}{T} \right) \right] + \dots$

Baryon diffusion coefficient $\kappa_B \propto C_B$ controls response of the diffusion current to the driving force.



Energy and baryon evolution in longitudinal direction (toy model) [Du et al. 1807.04721]

- Baryon diffusion leaves no pronounced signatures in the evolution of the energy density but **smoothes out gradients in baryon density** [Du & UH 1906.11181].
- An active topic:

[Monnai 1204.4713; Shen et al. 1704.04109; Moritz et al. 1711.08680; Denicol et al. 1804.10557; Li & Shen 1809.04034; ...].

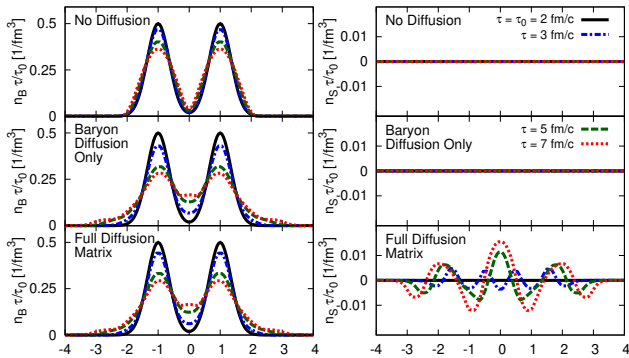
Mixed diffusion of multiple conserved charges

Coupled relaxation equations for the diffusion currents $i = B, Q, S$ [Fotakis et al. 1912.09103]:

$$u^\nu \partial_\nu n_i^\mu = -\frac{1}{\tau_n} \left[n_i^\mu - \kappa_{ij} \nabla^\mu \left(\frac{\mu_j}{T} \right) \right] + \dots$$

Common relaxation time τ_n for simplicity. Diffusion coefficient matrix κ_{ij} from kinetic theory.

Toy model with only longitudinal expansion (inviscid fluid, no transverse gradients):



Evolution of baryon and strangeness densities in longitudinal direction [Fotakis et al. 1912.09103]

Comparison with SPS and RHIC BES data

Hydrodynamic hybrid modeling of SPS and RHIC BES data

Here: focus on recent work from Chun Shen's group [Shen & Alzhrani 2003.05852] building on earlier papers [Shen & Schenke 1710.00881, Denicol et al. 1804.10557] but w/o dynamical initialization

(See also [Karpenko et al. 1502.01978, Monnai et al. 1902.05095].)

- Initial η_s profiles for energy and net baryon density from [Denicol et al. 1804.10557], but with **transverse profiles** for **energy density** $e(x, y) = M(x, y) \cosh(y_{CM}(x, y))$ and **longitudinal momentum density** $p_z(x, y) = M(x, y) \sinh(y_{CM}(x, y))$, with **invariant mass density** profile $M = m_n \sqrt{T_A^2 + T_B^2 + 2T_A T_B \cosh(2y_{beam})}$ ($\sim \sqrt{T_A T_B}$ for $\sqrt{s} > 5$ GeV) of the two colliding nuclear thickness functions T_A and T_B in the transverse plane.
- **Boost-invariant initial longitudinal flow profile** assumed.

Hydrodynamic hybrid modeling of SPS and RHIC BES data

Here: focus on recent work from Chun Shen's group [Shen & Alzhrani 2003.05852]

building on earlier papers [Chen & Schenke 1710.00881, Denicol et al. 1804.10557]

- Initial η_s profiles for energy and net baryon density from [Denicol et al. 1804.10557], but with **transverse profiles** for energy density

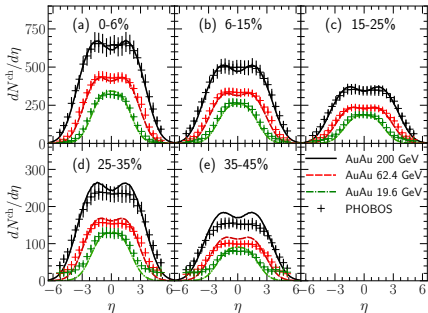
$$e(x, y) = M(x, y) \cosh(y_{CM}(x, y)) \text{ and}$$

$$\text{longitudinal momentum density } p_z(x, y) = M(x, y) \sinh(y_{CM}(x, y)), \text{ with}$$

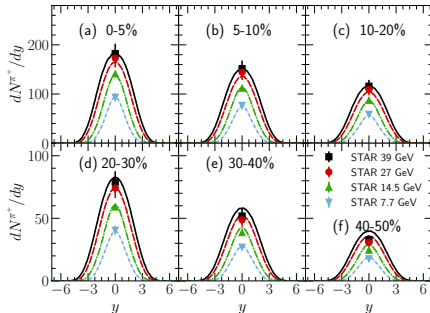
$$\text{invariant mass density profile } M = m_n \sqrt{T_A^2 + T_B^2 + 2T_A T_B \cosh(2y_{beam})} (\sim \sqrt{T_A T_B} \text{ for } \sqrt{s} > 5 \text{ GeV})$$

of the two colliding nuclear thickness functions T_A and T_B in the transverse plane.

charged hadron pseudorapidity distributions



pion rapidity distributions (RHIC)



Hydrodynamic hybrid modeling of SPS and RHIC BES data

Here: focus on recent work from Chun Shen's group [Shen & Alzhrani 2003.05852]

building on earlier papers [Chen & Schenke 1710.00881, Denicol et al. 1804.10557]

- Initial η_s profiles for energy and net baryon density from [Denicol et al. 1804.10557], but with **transverse profiles** for energy density

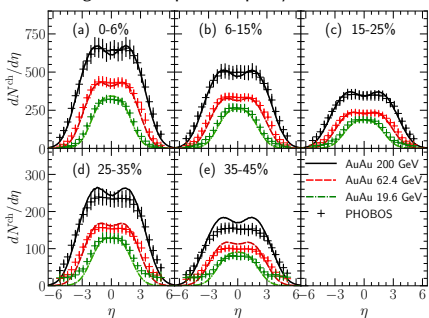
$$e(x, y) = M(x, y) \cosh(y_{CM}(x, y)) \text{ and}$$

$$\text{longitudinal momentum density } p_z(x, y) = M(x, y) \sinh(y_{CM}(x, y)), \text{ with}$$

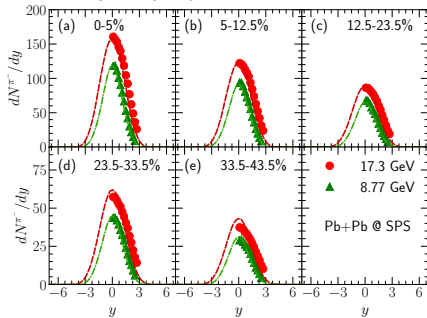
$$\text{invariant mass density profile } M = m_n \sqrt{T_A^2 + T_B^2 + 2T_A T_B \cosh(2y_{beam})} (\sim \sqrt{T_A T_B} \text{ for } \sqrt{s} > 5 \text{ GeV})$$

of the two colliding nuclear thickness functions T_A and T_B in the transverse plane.

charged hadron pseudorapidity distributions



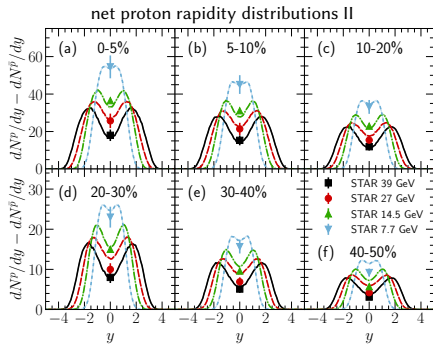
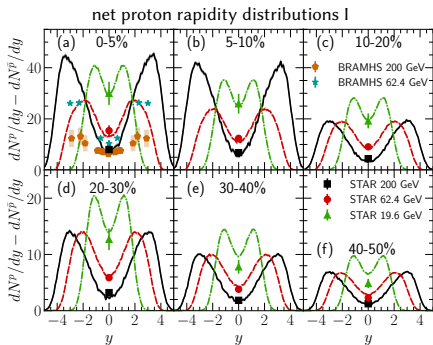
pion rapidity distributions (SPS)



Hydrodynamic hybrid modeling of SPS and RHIC BES data

Here: focus on recent work from Chun Shen's group [Shen & Alzhrani 2003.05852]
 building on earlier papers [Chen & Schenke 1710.00881, Denicol et al. 1804.10557]

- Initial η_s profiles for energy and net baryon density from [Denicol et al. 1804.10557], but with **transverse profiles** for energy density $e(x, y) = M(x, y) \cosh(y_{CM}(x, y))$ and longitudinal momentum density $p_z(x, y) = M(x, y) \sinh(y_{CM}(x, y))$, with invariant mass density profile $M = m_n \sqrt{T_A^2 + T_B^2 + 2T_A T_B \cosh(2y_{beam})}$ ($\sim \sqrt{T_A T_B}$ for $\sqrt{s} > 5$ GeV) of the two colliding nuclear thickness functions T_A and T_B in the transverse plane.



Hydrodynamic hybrid modeling of SPS and RHIC BES data

Here: focus on recent work from Chun Shen's group [Shen & Alzhrani 2003.05852]

building on earlier papers [Chen & Schenke 1710.00881, Denicol et al. 1804.10557]

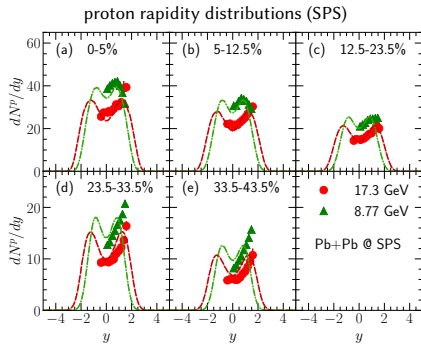
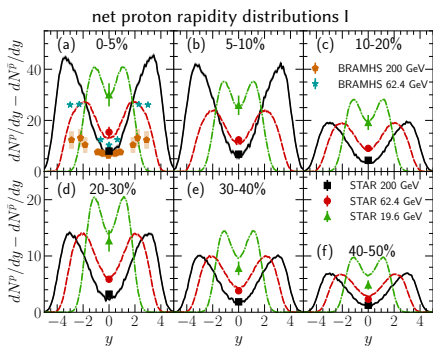
- Initial η_s profiles for energy and net baryon density from [Denicol et al. 1804.10557], but with **transverse profiles** for energy density

$$e(x, y) = M(x, y) \cosh(y_{CM}(x, y)) \text{ and}$$

$$\text{longitudinal momentum density } p_z(x, y) = M(x, y) \sinh(y_{CM}(x, y)), \text{ with}$$

$$\text{invariant mass density profile } M = m_n \sqrt{T_A^2 + T_B^2 + 2T_A T_B \cosh(2y_{beam})} (\sim \sqrt{T_A T_B} \text{ for } \sqrt{s} > 5 \text{ GeV})$$

of the two colliding nuclear thickness functions T_A and T_B in the transverse plane.



Hydrodynamic hybrid modeling of SPS and RHIC BES data

Here: focus on recent work from Chun Shen's group [Shen & Alzhrani 2003.05852]

building on earlier papers [Chen & Schenke 1710.00881, Denicol et al. 1804.10557]

- Initial η_s profiles for energy and net baryon density from [Denicol et al. 1804.10557], but with **transverse profiles** for

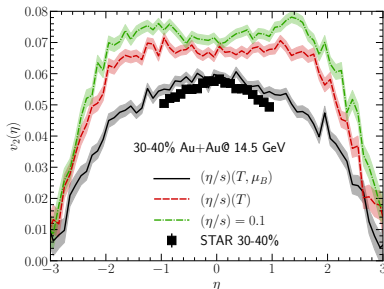
energy density $e(x, y) = M(x, y) \cosh(y_{CM}(x, y))$ and

longitudinal momentum density $p_z(x, y) = M(x, y) \sinh(y_{CM}(x, y))$, with

invariant mass density profile $M = m_n \sqrt{T_A^2 + T_B^2 + 2T_A T_B \cosh(2y_{beam})} (\sim \sqrt{T_A T_B} \text{ for } \sqrt{s} > 5 \text{ GeV})$

of the two colliding nuclear thickness functions T_A and T_B in the transverse plane.

charged hadron v_2 pseudorapidity distribution

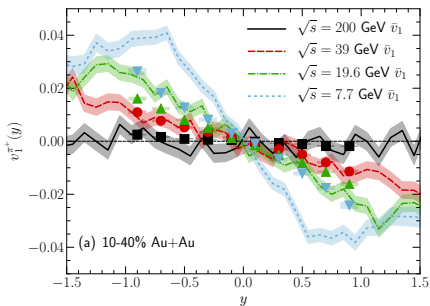


Hydrodynamic hybrid modeling of SPS and RHIC BES data

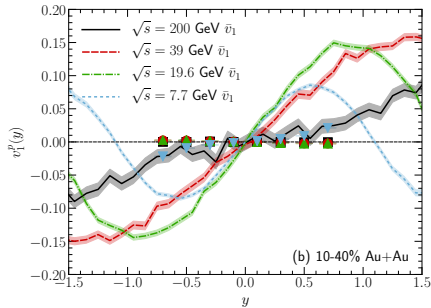
Here: focus on recent work from Chun Shen's group [Shen & Alzhrani 2003.05852]
 building on earlier papers [Chen & Schenke 1710.00881, Denicol et al. 1804.10557]

- Initial η_s profiles for energy and net baryon density from [Denicol et al. 1804.10557], but with **transverse profiles** for energy density $e(x, y) = M(x, y) \cosh(y_{CM}(x, y))$ and longitudinal momentum density $p_z(x, y) = M(x, y) \sinh(y_{CM}(x, y))$, with invariant mass density profile $M = m_n \sqrt{T_A^2 + T_B^2 + 2T_A T_B \cosh(2y_{beam})}$ ($\sim \sqrt{T_A T_B}$ for $\sqrt{s} > 5$ GeV) of the two colliding nuclear thickness functions T_A and T_B in the transverse plane.

pion v_1 rapidity distribution



proton v_1 rapidity distribution



Hydrodynamic hybrid modeling of SPS and RHIC BES data

Here: focus on recent work from Chun Shen's group [Shen & Alzhrani 2003.05852]

building on earlier papers [Chen & Schenke 1710.00881, Denicol et al. 1804.10557]

- Initial η_s profiles for energy and net baryon density from [Denicol et al. 1804.10557], but with **transverse profiles** for energy density $e(x, y) = M(x, y) \cosh(y_{\text{CM}}(x, y))$ and longitudinal momentum density $p_z(x, y) = M(x, y) \sinh(y_{\text{CM}}(x, y))$, with invariant mass density profile $M = m_n \sqrt{T_A^2 + T_B^2 + 2T_A T_B \cosh(2y_{\text{beam}})}$ ($\sim \sqrt{T_A T_B}$ for $\sqrt{s} > 5$ GeV) of the two colliding nuclear thickness functions T_A and T_B in the transverse plane.

- Many systematic features of hadron production data as functions of beam energy and collision centrality, transverse and longitudinal momentum are qualitatively well described by this approach.
- **Main failure:** rapidity distributions of (net) baryons and proton flow
- \implies **Need a better understanding of longitudinal initial conditions and baryon stopping!**

Hydro with critical fluctuations

Critical fluctuations and their off-equilibrium dynamics

- A critical point features **large fluctuations and correlations** [Gitterman *Rev. Mod. Phys.* 1978].

Dependence on the correlation length ξ stronger in higher-order cumulants (e.g. $K_3 \propto \xi^{4.5}$, $K_4 \propto \xi^7$).

Non-monotonic beam energy dependence of the normalized cumulants proposed as **telltale signature of the QCD critical point** [Stephanov 0809.3450 & 1104.1627; Bzdak et al. 1906.00936]:

Critical fluctuations and their off-equilibrium dynamics

- A critical point features **large fluctuations and correlations** [Gitterman *Rev. Mod. Phys.* 1978].
 Dependence on the correlation length ξ stronger in higher-order cumulants (e.g. $K_3 \propto \xi^{4.5}$, $K_4 \propto \xi^7$).
 Non-monotonic beam energy dependence of the normalized cumulants proposed as **telltale signature of the QCD critical point** [Stephanov 0809.3450 & 1104.1627; Bzdak et al. 1906.00936]:

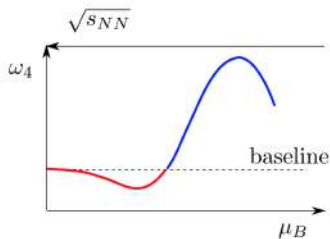
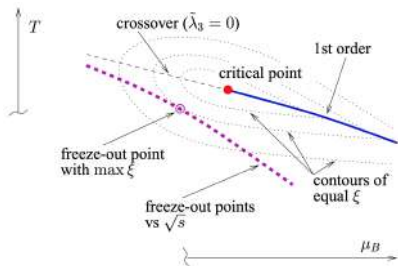


Illustration of the critical region and normalized quartic cumulant of proton multiplicity as a function of μ (proxy for $\sqrt{s_{NN}}$)

Critical fluctuations and their off-equilibrium dynamics

- A critical point features **large fluctuations and correlations** [Gitterman *Rev. Mod. Phys.* 1978].
 Dependence on the correlation length ξ stronger in higher-order cumulants (e.g. $K_3 \propto \xi^{4.5}$, $K_4 \propto \xi^7$).
 Non-monotonic beam energy dependence of the normalized cumulants proposed as **telltale signature of the QCD critical point** [Stephanov 0809.3450 & 1104.1627; Bzdak et al. 1906.00936]:

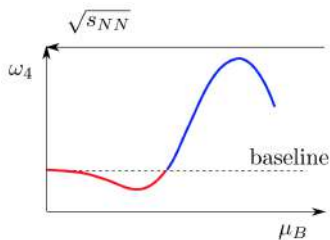
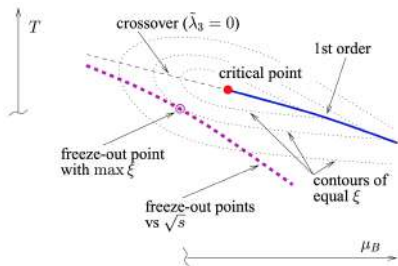


Illustration of the critical region and normalized quartic cumulant of proton multiplicity as a function of μ (proxy for $\sqrt{s_{NN}}$)

- Equilibration of such fluctuations is affected by **critical slowing-down** [Hohenberg & Halperin *Rev. Mod. Phys.* 1977].
 Since the QCD matter created in heavy-ion collisions **evolves very rapidly**, **off-equilibrium fluctuation effects become essential** [Berdnikov & Rajagopal hep-ph/9912274; Yi Yin 1811.06519];

Critical fluctuations and their off-equilibrium dynamics

- A critical point features **large fluctuations and correlations** [Gitterman *Rev. Mod. Phys.* 1978].
 Dependence on the correlation length ξ stronger in higher-order cumulants (e.g. $K_3 \propto \xi^{4.5}$, $K_4 \propto \xi^7$).
 Non-monotonic beam energy dependence of the normalized cumulants proposed as **telltale signature of the QCD critical point** [Stephanov 0809.3450 & 1104.1627; Bzdak et al. 1906.00936]:

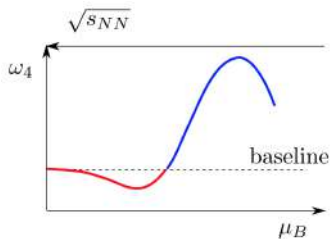
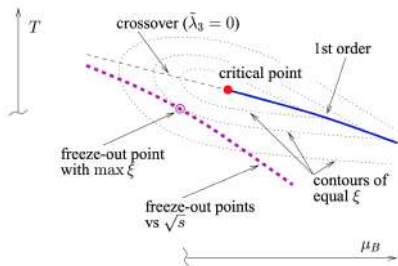


Illustration of the critical region and normalized quartic cumulant of proton multiplicity as a function of μ (proxy for $\sqrt{s_{NN}}$)

- Equilibration of such fluctuations is affected by **critical slowing-down** [Hohenberg & Halperin *Rev. Mod. Phys.* 1977].
 Since the QCD matter created in heavy-ion collisions **evolves very rapidly**, **off-equilibrium fluctuation effects become essential** [Berdnikov & Rajagopal hep-ph/9912274; Yi Yin 1811.06519];
- **Hydro+ framework**: conventional hydrodynamics coupled to slowly evolving critical modes.
 The **slowest mode** in the system created in heavy-ion collisions is $\delta(s/n)_p$ [Stephanov & Yin 1712.10305].

Critical fluctuations: equilibrium value

- Introduce phase-space density for the **slow degrees of freedom**, $\phi_{\mathbf{Q}}(\mathbf{x})$, via the Wigner transform of the two-point correlation of $\delta(s/n)_p$ [Stephanov & Yin 1712.10305; Xin An et al. 1902.09517, 1912.13456]:

$$\phi_{\mathbf{Q}}(\mathbf{x}) \sim \int_{\Delta\mathbf{x}} \left\langle \delta \frac{s}{n} \left(\mathbf{x} + \frac{\Delta\mathbf{x}}{2} \right) \delta \frac{s}{n} \left(\mathbf{x} - \frac{\Delta\mathbf{x}}{2} \right) \right\rangle e^{i\mathbf{Q} \cdot \Delta\mathbf{x}} .$$

- Define the **homogeneity length** ℓ of the fluid and the **correlation length** ξ as the typical length scales for variations of the 2-point correlator in \mathbf{x} and $\Delta\mathbf{x}$. **Hydro+ assumes the scale separation** $\ell \gg \xi$.

Critical fluctuations: equilibrium value

- Introduce phase-space density for the **slow degrees of freedom**, $\phi_Q(\mathbf{x})$, via the Wigner transform of the two-point correlation of $\delta(s/n)_p$ [Stephanov & Yin 1712.10305; Xin An et al. 1902.09517, 1912.13456]:

$$\phi_Q(\mathbf{x}) \sim \int_{\Delta\mathbf{x}} \left\langle \delta \frac{s}{n} \left(\mathbf{x} + \frac{\Delta\mathbf{x}}{2} \right) \delta \frac{s}{n} \left(\mathbf{x} - \frac{\Delta\mathbf{x}}{2} \right) \right\rangle e^{i\mathbf{Q} \cdot \Delta\mathbf{x}}.$$

- Define the **homogeneity length** ℓ of the fluid and the **correlation length** ξ as the typical length scales for variations of the 2-point correlator in \mathbf{x} and $\Delta\mathbf{x}$. **Hydro+ assumes the scale separation** $\ell \gg \xi$.
- In the **hydrodynamic limit** $Q=|\mathbf{Q}| \rightarrow 0$ the non-critical equilibrium value $\bar{\phi}_0$ is [Stephanov & Yin 1712.10305; Akamatsu et al. 1811.05081]

$$\bar{\phi}_0 = V \left\langle \left(\delta \frac{s}{n} \right)^2 \right\rangle = \frac{c_p}{n^2},$$

where $c_p = nT(\partial(s/n)/\partial T)_p$ is the **heat capacity**. $\bar{\phi}_0$ follows the medium evolution.

Critical fluctuations: equilibrium value

- Introduce phase-space density for the **slow degrees of freedom**, $\phi_Q(\mathbf{x})$, via the Wigner transform of the two-point correlation of $\delta(s/n)_p$ [Stephanov & Yin 1712.10305; Xin An et al. 1902.09517, 1912.13456]:

$$\phi_Q(\mathbf{x}) \sim \int_{\Delta\mathbf{x}} \left\langle \delta \frac{s}{n} \left(\mathbf{x} + \frac{\Delta\mathbf{x}}{2} \right) \delta \frac{s}{n} \left(\mathbf{x} - \frac{\Delta\mathbf{x}}{2} \right) \right\rangle e^{i\mathbf{Q} \cdot \Delta\mathbf{x}}.$$

- Define the **homogeneity length** ℓ of the fluid and the **correlation length** ξ as the typical length scales for variations of the 2-point correlator in \mathbf{x} and $\Delta\mathbf{x}$. **Hydro+ assumes the scale separation** $\ell \gg \xi$.
- In the **hydrodynamic limit** $Q=|\mathbf{Q}| \rightarrow 0$ the non-critical equilibrium value $\bar{\phi}_0$ is [Stephanov & Yin 1712.10305; Akamatsu et al. 1811.05081]

$$\bar{\phi}_0 = V \left\langle \left(\delta \frac{s}{n} \right)^2 \right\rangle = \frac{c_p}{n^2},$$

where $c_p = nT(\partial(s/n)/\partial T)_p$ is the **heat capacity**. $\bar{\phi}_0$ follows the medium evolution.

- In the **critical regime** ($Q \gg \xi^{-1}$), c_p is critically enhanced and the Q - and ξ -dependent **equilibrium value** is

$$\bar{\phi}_Q = \bar{\phi}_0 f_2(Q\xi) = \left[\left(\frac{c_p}{n^2} \right) \left(\frac{\xi}{\xi_0} \right)^2 \right] \frac{1}{1 + (Q\xi)^2},$$

where spatial isotropy for the Q -dependence is assumed. [Stephanov & Yin 1712.10305; Akamatsu et al. 1811.05081; Xin An et al. 1912.13456;

Rajagopal et al. 1908.08539]

Critical fluctuations: off-equilibrium dynamics

- The **slow-mode equations of motion** are of **relaxation form** [Stephanov & Yin 1712.10305; Akamatsu et al. 1811.05081; Xin An et al. 1912.13456]

$$u^\mu \partial_\mu \phi_Q = -\Gamma_Q (\phi_Q - \bar{\phi}_Q),$$

where u^μ is the flow velocity and $u^\mu \partial_\mu$ is the time-derivative in local rest frame.

Critical fluctuations: off-equilibrium dynamics

- The **slow-mode equations of motion** are of **relaxation form** [Stephanov & Yin 1712.10305; Akamatsu et al. 1811.05081; Xin An et al. 1912.13456]

$$u^\mu \partial_\mu \phi_Q = -\Gamma_Q (\phi_Q - \bar{\phi}_Q),$$

where u^μ is the flow velocity and $u^\mu \partial_\mu$ is the time-derivative in local rest frame.

- Close to the critical point, the Q -dependent **relaxation rate** Γ_Q is [Akamatsu et al. 1811.05081; Xin An et al. 1912.13456]

$$\Gamma_Q = \Gamma_\xi f_\Gamma(Q\xi) = \left[2 \left(\frac{\lambda_T}{c_p \xi^2} \right) \left(\frac{\xi_0}{\xi} \right)^2 \right] [(Q\xi)^2 (1 + (Q\xi)^2)],$$

where λ_T is the heat conductivity. Note **critical slowing down** as $\xi \rightarrow \infty$, and $\lim_{Q \rightarrow 0} \Gamma_Q = 0$.

Critical fluctuations: off-equilibrium dynamics

- The **slow-mode equations of motion** are of **relaxation form** [Stephanov & Yin 1712.10305; Akamatsu et al. 1811.05081; Xin An et al. 1912.13456]

$$u^\mu \partial_\mu \phi_Q = -\Gamma_Q (\phi_Q - \bar{\phi}_Q),$$

where u^μ is the flow velocity and $u^\mu \partial_\mu$ is the time-derivative in local rest frame.

- Close to the critical point, the Q -dependent **relaxation rate** Γ_Q is [Akamatsu et al. 1811.05081; Xin An et al. 1912.13456]

$$\Gamma_Q = \Gamma_\xi f_\Gamma(Q\xi) = \left[2 \left(\frac{\lambda_T}{c_p \xi^2} \right) \left(\frac{\xi_0}{\xi} \right)^2 \right] [(Q\xi)^2 (1 + (Q\xi)^2)],$$

where λ_T is the heat conductivity. Note **critical slowing down** as $\xi \rightarrow \infty$, and $\lim_{Q \rightarrow 0} \Gamma_Q = 0$.

- Dynamics of ϕ_Q controlled by competition between **macroscopic expansion** and **microscopic relaxation** processes, characterized by the “**critical Knudsen number**” ($\theta = \partial \cdot u =$ scalar expansion rate)

$$\text{Kn}(Q) \equiv \theta / \Gamma_Q.$$

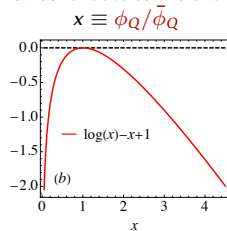
Slow modes with large critical Knudsen numbers will lag behind, not being able to follow the hydrodynamic evolution of the equilibrium value $\bar{\phi}_Q(x)$. [Berdnikov & Rajagopal hep-ph/9912274; Du et al. 2004.02719]

Critical fluctuations: back-reaction to the fluid

- The slow modes are additional, non-thermal degrees of freedom, which contribute to the **entropy density**, $s_{(+)}(e, n, \phi) \equiv s_{\text{eq}}(e, n) + \Delta s$, with [Stephanov & Yin 1712.10305]

$$\Delta s(e, n, \phi) = \int dQ \frac{Q^2}{(2\pi)^2} \left[\log \frac{\phi_Q}{\bar{\phi}_Q} - \frac{\phi_Q}{\bar{\phi}_Q} + 1 \right] < 0!$$

Note: Contribution from long-wavelength ($Q \rightarrow 0$) modes suppressed by phase space.

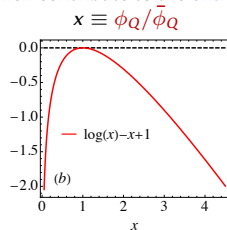


Critical fluctuations: back-reaction to the fluid

- The slow modes are additional, non-thermal degrees of freedom, which contribute to the **entropy density**, $s_{(+)}(e, n, \phi) \equiv s_{\text{eq}}(e, n) + \Delta s$, with [Stephanov & Yin 1712.10305]

$$\Delta s(e, n, \phi) = \int dQ \frac{Q^2}{(2\pi)^2} \left[\log \frac{\phi_Q}{\bar{\phi}_Q} - \frac{\phi_Q}{\bar{\phi}_Q} + 1 \right] < 0!$$

Note: Contribution from long-wavelength ($Q \rightarrow 0$) modes suppressed by phase space.



- They modify the inverse **temperature** and **chemical potential** of the bulk medium,

$$\beta_{(+)} = \left(\frac{\partial s_{(+)}}{\partial e} \right)_{n\phi} \equiv \frac{1}{T} + \Delta\beta, \quad \alpha_{(+)} = - \left(\frac{\partial s_{(+)}}{\partial n} \right)_{e\phi} \equiv \frac{\mu}{T} + \Delta\alpha,$$

and its **pressure** (“**back-reaction of non-equilibrium slow mode dynamics on the bulk**”):

$$p_{(+)} = (s_{(+)} - \beta_{(+)}e + \alpha_{(+)}n) / \beta_{(+)} \equiv p + \Delta p.$$

Slow-mode non-equilibrium dynamics in Gubser flow [Du et al. 2004.02719]

Medium evolution: externally prescribed **ideal Gubser flow** [Gubser 1006.0006] with **no back-reaction**.

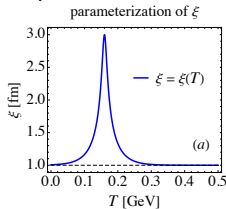
Temperature profile: $T(\tau, r) = C/(\tau \cosh^{2/3} \rho(\tau, r))$; other quantities from **conformal EoS** ($e \propto T^4$ and $n \propto T^3$).

Parametrization:

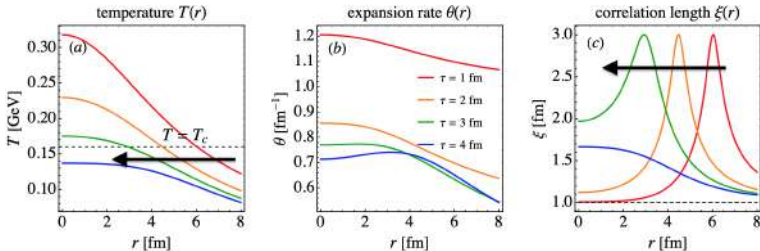
$$c_p = s^2 / ((\mu/T)n) \quad \text{[Akamatsu et al. 1811.05081]},$$

$\lambda_T \propto T^2$, and $\xi(T)$ from [Rajagopal et al. 1908.08539].

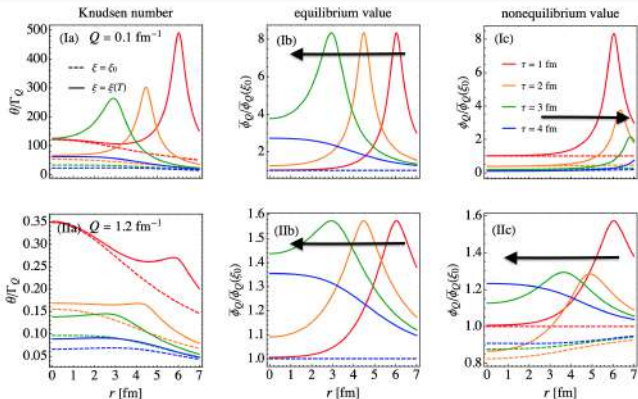
Gubser flow evolves at $\alpha = \mu/T = \text{const.}$



Snapshots of radial profiles for temperature $T(r)$, scalar expansion rate $\theta(r)$, correlation length $\xi(r)$:



Off-equilibrium slow-mode dynamics: expansion vs. thermalization



Dashed lines: $\xi = \xi_0$; solid lines: $\xi = \xi(T)$ [Du et al. 2004.02719]

- **Two counteracting effects at play:** (1) initial fluctuation peak gets carried outward by **advection** (through the $u^r \partial_r$ -term); (2) **relaxation** (through Γ_Q) towards the inward-moving equilibrium peak drags the fluctuation peak inward (hampered by critical slowing-down).
- For **small- Q modes** ($Q < \xi_{\max}^{-1}$) with **large $\text{Kn}(Q)$** , thermalization is slow and **advection** wins over **relaxation** (top row); *vice versa* for **large- Q modes** ($Q \gg \xi_{\max}^{-1}$) with **small $\text{Kn}(Q)$** (bottom row).

- Equation of motion:

$$(u^r \partial_\tau + u^r \partial_r) \phi_Q = -\Gamma_Q (\phi_Q - \bar{\phi}_Q)$$

- Equilibrium initial conditions:

$$\phi_Q(\tau_0) = \bar{\phi}_Q(\tau_0) \text{ at } \tau_0 = 1 \text{ fm}/c$$

- Note: equilibrium value $\bar{\phi}_Q$ is evolving and a “moving target” for ϕ_Q

Non-equilibrium fluctuation dynamics: feedback on entropy density

- Critical slow-mode dynamics:

$$(u^\tau \partial_\tau + u^r \partial_r) \phi_Q = -\Gamma_Q (\phi_Q - \bar{\phi}_Q)$$

Equilibrium value $\bar{\phi}_Q$:

$$\bar{\phi}_Q = \left[\left(\frac{c_p}{n^2} \right) \left(\frac{\xi}{\xi_0} \right)^2 \right] f_2(Q\xi)$$

Relaxation rate Γ_Q :

$$\Gamma_Q = \left[2 \left(\frac{\lambda_T}{c_p \xi^2} \right) \left(\frac{\xi_0}{\xi} \right)^2 \right] f_\Gamma(Q\xi).$$

Advection, critical growth of ξ , and medium evolution of n , c_p , λ_T can be turned off and on and effects studied separately [Du et al. 2004.02719].

Non-equilibrium fluctuation dynamics: feedback on entropy density

- Critical slow-mode dynamics:

$$(u^\tau \partial_\tau + u^r \partial_r) \phi_Q = -\Gamma_Q (\phi_Q - \bar{\phi}_Q)$$

Equilibrium value $\bar{\phi}_Q$:

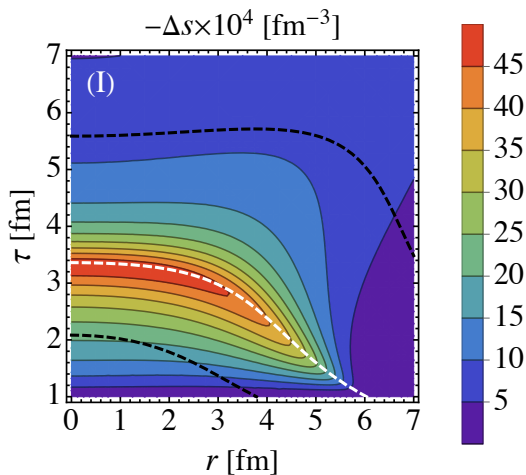
$$\bar{\phi}_Q = \left[\left(\frac{c_p}{n^2} \right) \left(\frac{\xi}{\xi_0} \right)^2 \right] f_2(Q\xi)$$

Relaxation rate Γ_Q :

$$\Gamma_Q = \left[2 \left(\frac{\lambda_T}{c_p \xi^2} \right) \left(\frac{\xi_0}{\xi} \right)^2 \right] f_\Gamma(Q\xi).$$

Advection, critical growth of ξ , and medium evolution of n , c_p , λ_T can be turned off and on and effects studied separately [Du et al. 2004.02719].

- Overall feedback effect is tiny (see figure at right): $\Delta s / s_{\text{eq}} \sim \mathcal{O}(10^{-4})$.



Space-time evolution of non-equilibrium correction to the entropy density

Non-equilibrium fluctuation dynamics: feedback on eccentricities

- Study linearized anisotropic deformations of Gubser profile at early time $\tau \ll 1/q$ [Hatta et al. 1405.1984 & 1505.04226]:

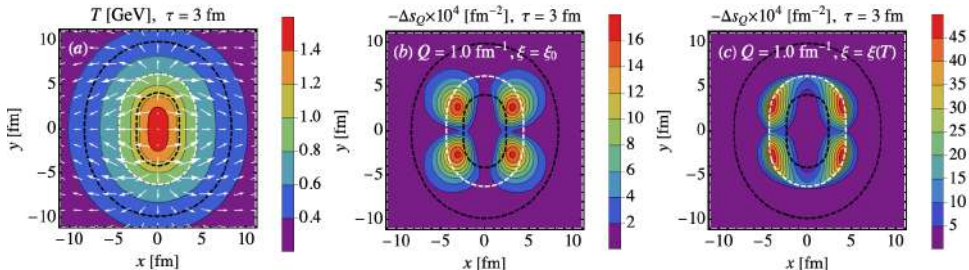
$$T_{\text{iso}} \approx \frac{C}{\tau^{1/3}} \frac{(2q)^{2/3}}{(1+q^2r^2)^{2/3}}, \quad T(\tau, r, \phi) = T_{\text{iso}}(1 - \epsilon_n \mathcal{A}_n \delta), \quad \mathcal{A}_n \equiv \left(\frac{2qr}{1+(qr)^2} \right)^n \cos(n\phi).$$

Non-equilibrium fluctuation dynamics: feedback on eccentricities

- Study linearized anisotropic deformations of Gubser profile at early time $\tau \ll 1/q$ [Hatta et al. 1405.1984 & 1505.04226]:

$$T_{\text{iso}} \approx \frac{C}{\tau^{1/3}} \frac{(2q)^{2/3}}{(1 + q^2 r^2)^{2/3}}, \quad T(\tau, r, \phi) = T_{\text{iso}}(1 - \epsilon_n \mathcal{A}_n \delta), \quad \mathcal{A}_n \equiv \left(\frac{2qr}{1 + (qr)^2} \right)^n \cos(n\phi).$$

- Shown is $n = 2$ (ellipticity). Largest corrections to entropy from non-equilibrium fluctuations arise at points of largest expansion rate, further enhanced by large correlation length:



(a): Temperature and flow profile for $\epsilon_2 = 0.15$. (b,c): Δs_Q with $\xi = \xi_0$ (b) and with $\xi = \xi(T)$ (c). [Du et al. 2004.02719].

- Overall feedback effect from non-eq. slow mode dynamics is **tiny increase of the ellipticity** ($\delta\epsilon_2/\epsilon_2 < 10^{-4}$).

Limits of the Hydro+ framework

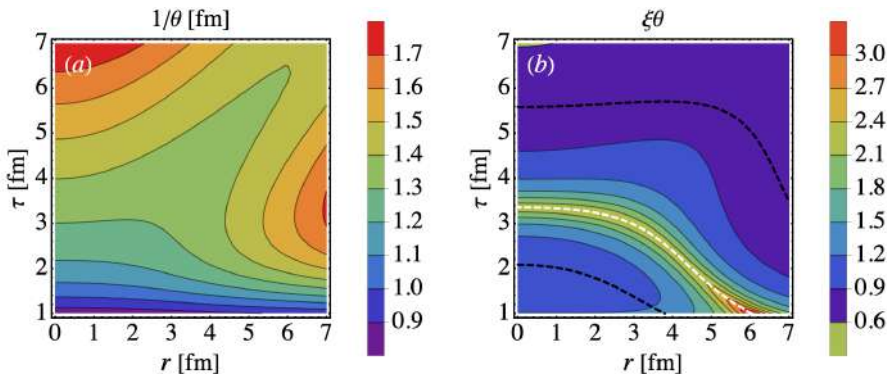
- Fundamental assumption of Hydro+: scale separation $\ell \gg \xi$
(ξ = correlation length, ℓ = hydrodynamic homogeneity length);

Limits of the Hydro+ framework

- **Fundamental assumption of Hydro+:** scale separation $\ell \gg \xi$
(ξ = correlation length, ℓ = hydrodynamic homogeneity length);
- (1+1)-d Gubser flow has effectively only **one macroscopic length scale parameter:** $\ell \sim 1/\theta$.
Scale separation thus requires $\xi/\ell \sim \xi\theta < \mathcal{O}(1)$.

Limits of the Hydro+ framework

- Fundamental assumption of Hydro+: scale separation $\ell \gg \xi$ (ξ = correlation length, ℓ = hydrodynamic homogeneity length);
- (1+1)-d Gubser flow has effectively only one macroscopic length scale parameter: $\ell \sim 1/\theta$. Scale separation thus requires $\xi/\ell \sim \xi\theta < \mathcal{O}(1)$.



(a) hydrodynamic homogeneity length ℓ ; (b) $\xi/\ell \sim \xi\theta$ [Du et al. 2004.02719]

- Hydro+ framework gets **most strongly challenged close to the critical point.**

Conclusions

Conclusions

■ Part I: Dissipative hydrodynamics at non-zero net baryon density

- Hydrodynamics at low collision energies requires (3+1)D dynamical initialization and evolution with EoS at nonzero conserved charge densities. Much recent progress along this direction, but baryon stopping and 3-d initial conditions for baryon density still major source of theoretical uncertainty.
- Baryon diffusion affects specifically baryonic observables and should thus be included in hydrodynamic simulations for Beam Energy Scan studies; non-baryonic observables (e.g. total charged multiplicity distributions) are insensitive to baryon diffusion.
- BESHYDRO is designed for this purpose and well documented.

■ Part II: Fluctuation dynamics near the QCD critical point

- Different aspects of the off-equilibrium dynamics controlling the evolution of critical fluctuations have been analyzed. Important Q -dependent competition between advection and relaxation (thermalization).
- Back-reaction effects from off-equilibrium critical slow-mode dynamics on bulk evolution appear to be unmeasurably small.

Thank you very much!